PHYSICAL REVIEW B **90**, 201305(R) (2014)

Excitonic ring formation in ultrapure bulk GaAs

S. Bieker, T. Henn, T. Kiessling,* W. Ossau, and L. W. Molenkamp
Physikalisches Institut (EP3) der Universität Würzburg, 97074 Würzburg, Germany
(Received 7 May 2014; revised manuscript received 8 October 2014; published 10 November 2014)

We report on spatially resolved low-temperature photoluminescence (PL) measurements of excitons in ultrapure bulk GaAs. At moderate excitation densities we observe butterfly-shaped luminescence images in the wavelength–radial distance plane with a pronounced quench of the exciton PL intensity at the excitation center. The shapes of the PL images show a delicate dependence on excitation wavelength and pump power. We present a model that quantitatively explains the PL intensity quench by a localized overheating of the exciton ensemble due to nonresonant optical excitation. Our model allows us to extract absolute exciton temperatures and to trace the influence of excitation excess energy on the spatial dependence of the exciton energy relaxation. We observe temperature gradients in the exciton system which persist over distances $\geqslant 10$ μm away from the excitation spot.

DOI: 10.1103/PhysRevB.90.201305 PACS number(s): 78.55.Cr, 71.35.−y, 78.20.−e

The first observation of macroscopic concentric PL rings from indirect excitons in electrically gated double quantum wells (QWs) [1,2] initiated a series of insightful spatially resolved photoluminescence (SRPL) studies on these structures. While the periodic fragmentation of the outer ring seen at low lattice temperatures is assumed to hint towards a macroscopically ordered phase of the excitons [2–4], the very fact of inner and outer ring formation has found simpler explanations. The outer ring was shown to originate from a spatial separation of the electron and hole plasma in the quantum well [3,5]. The inner halo turned out to result from a temperature gradient within the exciton gas. Surprisingly, for SRPL measurements on bulk semiconductors, excitonic ring formation due to a local overheating of the exciton system with respect to the lattice has not been reported yet.

In this Rapid Communication we show that a temperature effect conceptually similar to the inner ring formation in indirect QWs emerges in SRPL spectra of ultrapure bulk GaAs. At moderate excitation densities we observe butterfly-shaped luminescence images in the wavelength–radial distance plane with a pronounced quench of the exciton PL at the excitation center. We present a quantitative model for this local quenching of the PL emission intensity by an overheating of the exciton ensemble upon nonresonant optical excitation. Our model allows us to directly trace the influence of excitation excess energy on the spatially dependent exciton energy relaxation. We observe temperature gradients in the exciton system which persist over distances $\geqslant 10$ μm, which exceeds the size of the excitation laser spot by an order of magnitude.

All results presented in this Rapid Communication are obtained on an unintentionally n-doped, 70 μm thick layer of (001)-oriented liquid phase epitaxy (LPE) grown GaAs. The sample is mounted on the cold finger of a liquid helium flow optical cryostat equipped with a calibrated Cernox resonant-tunneling diode temperature sensor placed next to the sample for accurate temperature control. All measurements are performed at 5.5 K lattice temperature. Tunable optical excitation is provided by a continuous wave Ti:sapphire laser. The beam is focused on the sample surface by an infinity-corrected NA = 0.4 microscope objective to a $(1/e)$ spot diameter of 3.6 μm. Luminescence is collected in confocal geometry, focused on the entrance slit of a 1 m focal length monochromator equipped with a 1200 mm^{-1} grating, and detected by a liquid-nitrogen-cooled CCD array. Spatial information on the local PL intensity is contained in the vertical pixel number of the two-dimensional CCD image.

The near band edge PL spectrum under defocused optical excitation is displayed in Fig. 1(a) with the usual assignment of free and bound exciton transitions [6]. Unambiguous assignment of the 8192 Å line mandates additional characterization since both the recombination of excitons bound to ionized donor sites (D^+,X) and the neutral donor-hole transition (D^0,h) appear at the same energetic position in the spectrum [7]. In time-resolved PL measurements, we observe identical decay times of (5.0 ± 0.4) ns on the (D^0,X) and (D^+,X) transition and conclude that in our sample, the 8192 Å line is of predominantly excitonic origin. Our model results will later corroborate this interpretation.

We show in Figs. 1(b) and 1(c) representative CCD images obtained under focused laser excitation where a characteristic butterfly shape of the luminescence images appears in the wavelength–radial distance plane. At short-wavelength optical excitation ($\lambda_{exc} = 7830$ Å), a pronounced quench of the bound exciton luminescence is seen at the excitation center. The luminescence images undergo a marked transformation when the excitation wavelength λ_{exc} is tuned towards the GaAs band gap. The dip at the excitation center gradually diminishes and the butterfly wings ultimately merge into a luminescence image with bell-shaped spatial PL profiles at all detection wavelengths ($\lambda_{exc} = 8130$ Å).

This transformation is displayed in more detail in Figs. 2(a) and 2(b) where we show vertical line cuts at 8188 Å and 8192 Å, which yield spatial PL profiles of the (D^0,X) and (D^+,X) transitions as a function of excitation wavelength. Figure 2(c) reveals a similar transformation of the PL profiles as a function of pump power for a fixed excitation wavelength ($\lambda_{exc} = 7850$ Å): Bell-shaped PL profiles are observed in the weak-excitation limit. When the pump intensity is increased, the profiles flatten and a dip around the photoexcitation spot appears which saturates for large P_{exc}. No PL quench at the center of excitation is observed at elevated sample

*tobias.kiessling@physik.uni-wuerzburg.de

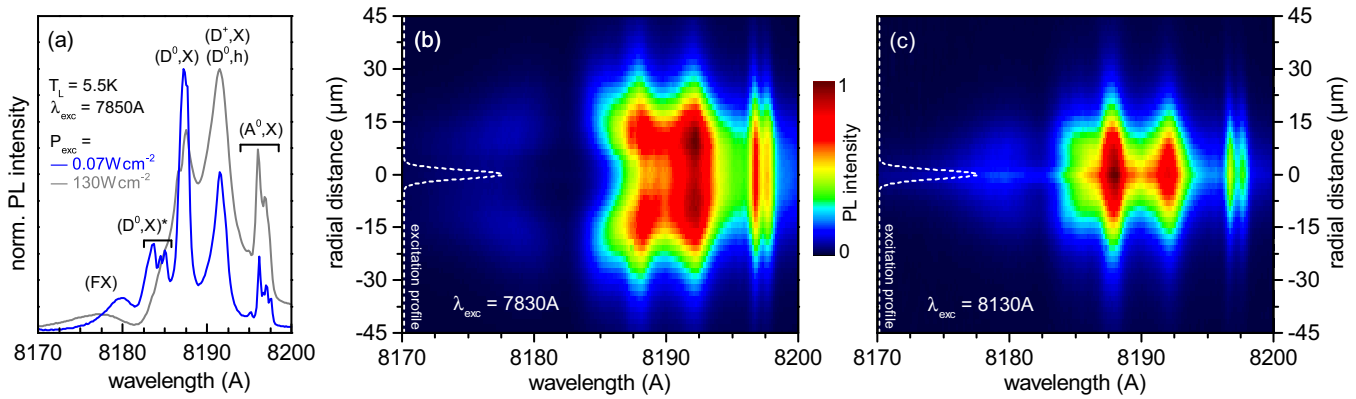

FIG. 1. (Color online) (a) Excitonic PL spectrum of the ultrapure bulk GaAs sample at different optical excitation densities. Text labels indicate the usual nomenclature of free and bound exciton transitions [6]. (b) Spatially resolved PL images revealing the characteristic butterfly shape in the wavelength–radial distance plane. Note the marked transformation of the luminescence image when the excitation wavelength is tuned closer towards the fundamental GaAs band gap (c). Both PL images are obtained under equal excitation power of 700 μW. Dashed Gaussians indicate the spatial intensity profile of the monochromatic excitation laser with a 3.6 μm ($1/e$) spot diameter.

temperatures $T_L \geqslant 12$ K, irrespective of pump power and excitation wavelength.

The distinctive dependence of the PL images on excitation wavelength unambiguously rules out lattice heating and exciton screening by an electron hole plasma as possible explanations for the local luminescence quench. Instead, the dependence on pump power, excitation wavelength, and lattice temperature is characteristic for heating effects in the photocarrier system. We therefore suggest that the PL quench at the excitation center is due to an overheating of the exciton ensemble caused by nonresonant optical excitation.

In contrast to the electron temperature, which in bulk semiconductors can be directly read from the PL line shape of the electron-to-neutral-acceptor transition (e, A^0) [8], a direct

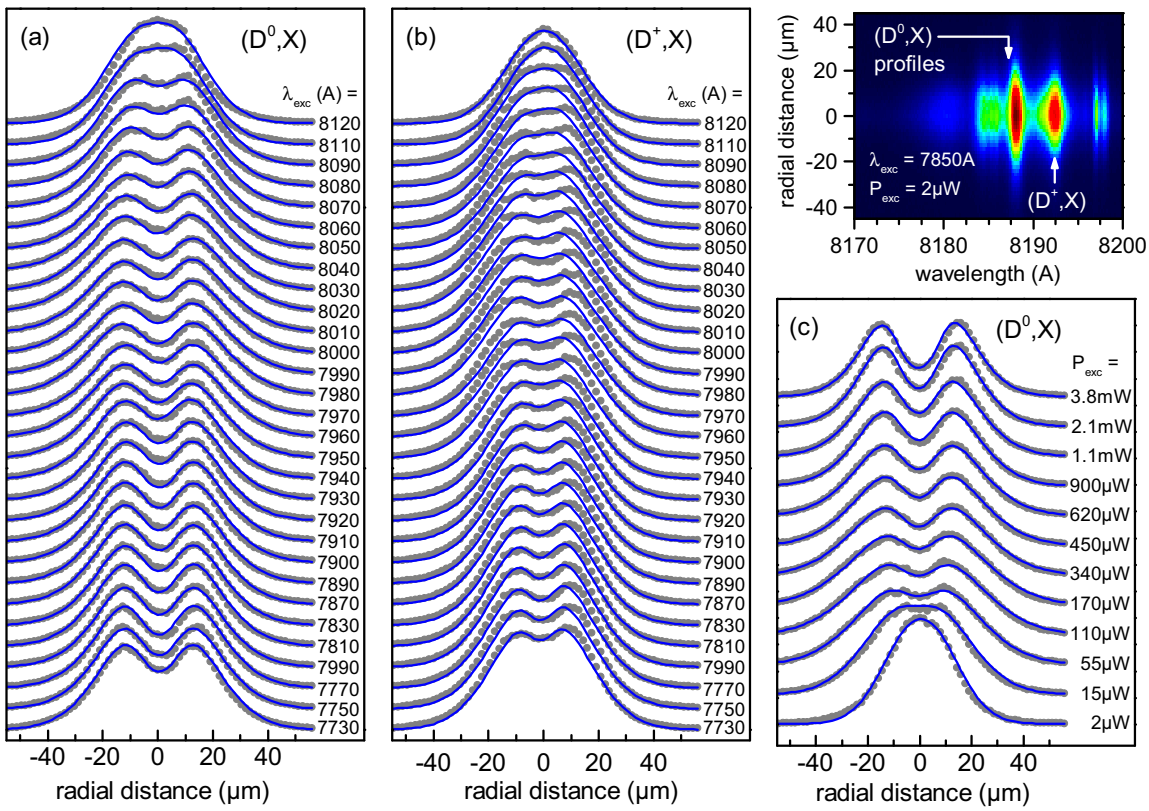

FIG. 2. (Color online) (a), (b) Spatially resolved PL profiles of excitons recombining at neutral (D^0, X) and ionized donor sites (D^+, X) for different excitation wavelengths at fixed $P_{\text{exc}} = 700$ μW. (c) Transformation of the (D^0, X) PL profiles as a function of pump power at fixed $\lambda_{\text{exc}} = 7850$ Å. Our model (solid blue lines) reproduces all details of the experimental data and allows us to determine the exciton temperature at the excitation center from the depth of the PL quench. Extracted values for T_X at the center of excitation are displayed in Figs. 4(c) and 4(d) as a function of excitation wavelength and optical pump power.

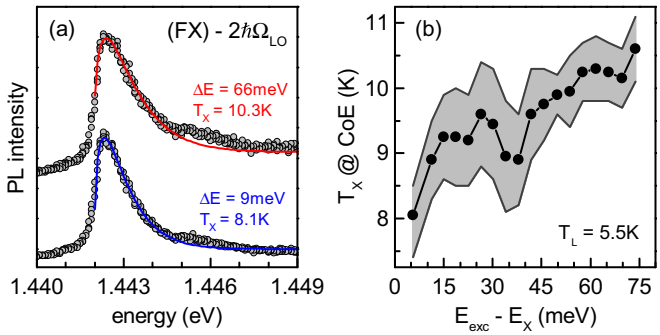

FIG. 3. (Color online) (a) PL spectra of the $(FX) - 2\hbar\Omega_{\mathrm{LO}}$ replica with Maxwellian fits to the line shape to determine T_X at the center of excitation (CoE). (b) T_X as a function of excitation excess energy. Note the systematic error caused by the spurious PL background, which is indicated by the gray shading.

measurement of the *exciton temperature* T_X is difficult. The two-branch dispersion relation for the coupled exciton-photon modes leads to a nontrivial line shape of the (FX) transition [9]. For $T_X \leqslant 15$ K it is therefore not possible to infer the temperature of excitons in bulk semiconductors from their radiative recombination line shape [7]. Only the second LO-phonon replica $(FX) - 2\hbar\Omega_{\mathrm{LO}}$ of the free exciton transition is known to mirror the Maxwellian energy distribution of a thermalized exciton ensemble [10,11]. Its very weak emission intensity, however, is a major obstacle to a direct mapping of $T_X(r)$ for large distances r from the excitation spot.

To verify the assumption of a local exciton overheating we measure the emission of the $(FX) - 2\hbar\Omega_{\mathrm{LO}}$ replica at the center of optical excitation where sufficient PL intensity is detected. Maxwellian line shape fits to the data are shown in Fig. 3(a) for exemplary excitation energies. We note that the second phonon replica is not perfectly isolated in the luminescence spectrum. Nearby defect-related transitions and presumably the $(FX) - 2\hbar\Omega_{\mathrm{TO}}$ replica cause a spectrally broad spurious PL background which cannot be exactly quantified. The assumption which we make for this background introduces a systematic error in the temperature determination, the range of which is indicated in Fig. 3(b) by the gray shading.

Figure 3, however, unambiguously demonstrates a local overheating of the nonresonantly excited excitons. T_X significantly exceeds the lattice temperature at the excitation center and increases for increasing excitation excess energies. We next present a model, based on a localized exciton overheating, which enables a quantitative analysis of the spatial PL profiles. We will later show that this model allows for a more precise determination of the exciton temperature.

The model anticipates the following physical picture: hot excitons are generated by the focused laser beam and diffuse away from the excitation region, meanwhile relaxing their excess energy by emission of phonons and scattering with lower energy excitons and charge carriers [12]. A steady-state situation builds up with radially symmetric exciton density and temperature gradients. At each distance r from the excitation spot, we describe the emitted PL intensity by the product $I(r) \propto n_X(r) \times \xi\,[T_X(r)]$ with the local free exciton

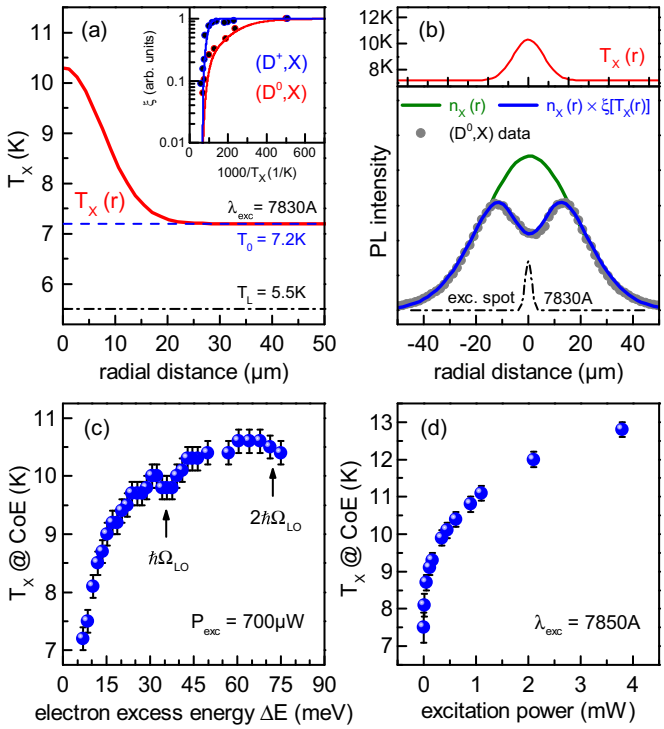

FIG. 4. (Color online) (a) Model for a localized overheating of the exciton ensemble near the photoexcitation spot. Deviation of T_0 from T_L is a result of incomplete excess energy relaxation of the excitons within their radiative lifetime. The inset shows data points from Ref. [7] together with a fit assuming two activation energies of 7 and 1 meV. (b) Exemplary illustration of the analysis procedure: $n_X(r)$ is adjusted to the outer wings of the measured PL profiles. Fitting $\xi\,[T_X(r)] \times n_X(r)$ to the data yields estimates for the width and amplitude of the overheating. A distinct PL quench only emerges when $n_X(r)$ is broader than $T_X(r)$. (c) Exciton temperature T_X at the center of excitation (CoE) obtained from the model as a function of electron excess energy and (d) as a function of pump power.

density $n_X(r)$ and a temperature-dependent occupation factor $\xi\,[T_X(r)]$ specific to each recombination path.

We first consider the occupation factor $\xi\,[T_X(r)]$. For the analysis presented in this Rapid Communication, we restrict ourselves to the recombination of excitons localized at neutral and ionized donor sites for which reliable information on $\xi(T)$ is available in the literature. The emission intensities of the (D^0,X) and (D^+,X) lines are studied in detail in Ref. [7] as a function of lattice temperature. The authors find a pronounced quenching of the PL intensity for increasing sample temperatures with two characteristic dissociation energies of 7 meV and 1 meV. Data points from Ref. [7] are shown in the inset of Fig. 4(a) as black circles. We interpret these PL intensity quenches as temperature dependent localization probabilities of free excitons at the respective donor sites and therefore conclude that the temperature relevant to this process is not that of the lattice, but T_X. We take the empirical expressions for the temperature quenches with the activation energies provided in Ref. [7] as an approximation for the occupation factors $\xi\,[T_X(r)]$ in our model.

For the spatial dependence of the exciton temperature $T_X(r)$, we assume as a first approximation a Gaussian-shaped

overheating of the exciton ensemble peaked at the center of optical excitation [see Fig. 4(a)]. The width and peak amplitude of $T_X(r)$ are determined in the following by fitting our model to the PL intensity profiles. The temperature T_0 far away from the excitation spot is not set to the lattice temperature T_L as one might expect at first, but to the respective value obtained from Maxwellian line shape fits to the $(FX) - 2\hbar\Omega_{\mathrm{LO}}$ replica measured under defocused weak excitation using the same laser wavelength. We find that the spurious luminescence background which complicates the analysis under focused excitation is considerably reduced in the weak-excitation limit which therefore here allows for a precise determination of T_X. The deviation of T_0 from T_L occurs because nonresonantly excited excitons cannot fully thermalize with the crystal lattice within their short lifetime.

We next consider the exciton density profile $n_X(r)$. Because only excitons with wave vectors matching that of the emitted photon can recombine radiatively, the spatially resolved (FX) intensity may not be taken as a direct measure for n_X [13]. As an empirical approximation for $n_X(r)$, we instead fit Gaussian envelopes to the outer wings of the measured (D^0,X) PL profiles assuming that the bound exciton luminescence is proportional to n_X outside the overheating region. We carefully ruled out any artificial flattening of the $n_X(r)$ profiles due to saturation of the low residual donor density even at the highest excitation power. All building blocks of our model are summarized in Figs. 4(a) and 4(b).

The two free model parameters left are the width and amplitude of the exciton temperature profile. Fitting our model to the measured (D^0,X) profile at 7730 Å excitation wavelength yields a $T_X(r)$ Gaussian with 10.4 K peak temperature and an $(1/e)$ full width of 21 μm. For all other excitation wavelengths, the $T_X(r)$ width is kept fixed at this value. Since T_0 is individually determined experimentally for each λ_{exc}, the overheating amplitude remains the only variable parameter.

A comparison between the experimentally determined (D^0,X) profiles and our model is displayed in Fig. 2. Our model allows us to reproduce all details of the PL profiles for the whole set of excitation wavelengths [Fig. 2(a)] and for all pump powers [Fig. 2(c)] by only adjusting the overheating amplitude. Furthermore, with the expression for the (D^+,X) occupation factor from the literature and the exact same temperature profile $T_X(r)$ as for the model description of the (D^0,X) line, we also find very good agreement between the (D^+,X) PL profiles and our model predictions for the whole set of excitation wavelengths [Fig. 2(b)]. We emphasize that once $T_X(r)$ is fixed from the analysis of the (D^0,X) profiles, no free parameter is left to adjust the (D^+,X) model to the experimental data. We regard the very good agreement as strong evidence that our model captures the essential physics underlying the bound exciton ring formation. The model result furthermore supports our previous interpretation that the main contribution to the 8192 Å line is due to excitons recombining at ionized donor sites.

The results of our analysis are summarized in Figs. 4(c) and 4(d), which display the peak exciton temperature as a function of excitation excess energy and pump power. We show in Fig. 4(c) that the $T_X(r=0)$ peak amplitude increases for decreasing excitation wavelength λ_{exc} (increasing photon energies E_{Ph}). The peak exciton temperatures obtained from our model agree quantitatively with the values independently determined from the line shape analysis of the $(FX) - 2\hbar\Omega_{\mathrm{LO}}$ transition shown in Fig. 3(b). The observed excitation excess energy dependence points towards the microscopic mechanism of excess energy dissipation following nonresonant optical excitation. A deviation of the increasing T_X trend is seen when the *electron* excess energy [14] $\Delta E = (E_{\mathrm{Ph}} - E_G) \times (1 + m_e/m_h)^{-1}$ coincides with the GaAs LO phonon energy $\hbar\Omega_{\mathrm{LO}} = 36$ meV. This nonmonotonic excess energy dependence $T_X(\Delta E)$ is characteristic of photocarrier heating [15]: Integer multiples of $\hbar\Omega_{\mathrm{LO}}$ electron excess energy are efficiently relaxed by rapid LO phonon emission, which happens on a faster time scale than the subsequent exciton formation. The replication of the dip at $2 \times \hbar\Omega_{\mathrm{LO}}$ is not fully resolved because of the limited tuning range of our pump laser.

Figure 4(d) displays the saturation of the $T_X(r)$ peak temperature as a function of pump power, a behavior that is also characteristic of photocarrier heating [16] and further supports our interpretation of the bound exciton ring formation.

In addition to probing the exciton temperature at the excitation center, our model allows us to observe the spatial energy relaxation of optically excited excitons. We find that the slow time scale for the residual excess energy relaxation via acoustic phonons [13] results in the buildup of significant exciton temperature gradients which persist over macroscopic length scales. Our analysis demonstrates that the local overheating of the excitons persists over $\geqslant 10$ μm, which exceeds the spatial extent of the pump source by an order of magnitude. Even far from the excitation spot, full thermalization with the crystal lattice is not reached due to the competing time scales of energy relaxation and radiative recombination.

We conclude by noting that overheating effects due to insufficient energy relaxation of optically excited excitons are present in all low-temperature experiments involving nonresonant optical exciton generation. However, the clear direct manifestation of the exciton overheating as butterfly-shaped PL profiles with a luminescence quench at the excitation center is only observable in nearly defect-free bulk samples with ultrahigh carrier mobilities. Here the exceptionally long diffusion lengths lead to $n_X(r)$ profiles which are wider than the $T_X(r)$ distribution. In the framework of the presented model, this condition is required for the excitonic ring formation.

We have checked the applicability of our model to other high-purity GaAs samples. We found qualitatively similar results for unintentionally *p*-doped reference samples of LPE grown bulk GaAs and ultrapure molecular beam epitaxy (MBE) grown GaAs epilayers. In all samples, even larger peak temperatures up to 20 K were observed, indicating higher residual impurity concentrations in these samples [13].

ACKNOWLEDGMENTS

The excellent GaAs sample was provided by E. Bauser. The authors gratefully acknowledge support by the DFG (SPP 1285 OS98/9-3) and the ERC (AG 3-TOP).

[1] D. Snoke, S. Denev, Y. Liu, L. Pfeiffer, and K. West, Nature (London) **418**, 754 (2002).
[2] L. V. Butov, A. C. Gossard, and D. S. Chemla, Nature (London) **418**, 751 (2002).
[3] L. V. Butov, L. S. Levitov, A. V. Mintsev, B. D. Simons, A. C. Gossard, and D. S. Chemla, Phys. Rev. Lett. **92**, 117404 (2004).
[4] S. V. Andreev, A. A. Varlamov, and A. V. Kavokin, Phys. Rev. Lett. **112**, 036401 (2014).
[5] R. Rapaport, G. Chen, D. Snoke, S. H. Simon, L. Pfeiffer, K. West, Y. Liu, and S. Denev, Phys. Rev. Lett. **92**, 117405 (2004).
[6] M. R. Brozel and G. E. Stillmann (eds.), *Properties of Gallium Arsenide*, 3rd ed. (Institution of Electrical Engineers, London, 1996).
[7] E. Bogardus and H. Bebb, Phys. Rev. **176**, 993 (1968).
[8] D. M. Eagles, J. Phys. Chem. Solids **16**, 76 (1960).
[9] J. Hopfield, Phys. Rev. **112**, 1555 (1958).
[10] E. Gross, S. Permogorov, and B. Razbirin, J. Phys. Chem. Solids **27**, 1647 (1966).
[11] B. Segall and G. Mahan, Phys. Rev. **171**, 935 (1968).
[12] J. Shah, *Ultrafast Spectroscopy of Semiconductors and Semiconductor Nanostructures*, Springer Series in Solid-State Sciences (Springer, 1999).
[13] S. Permogorov, Phys. Status Solidi B **68**, 9 (1975).
[14] $E_G = 1.519$ eV is the fundamental GaAs band gap and $m_e = 0.067m_0$ ($m_h = 0.51m_0$) the GaAs electron (hole) effective masses with $m_0 = 9.11 \times 10^{-31}$ kg the free electron mass.
[15] C. Weisbuch, Solid-State Electron. **21**, 179 (1978).
[16] J. Shah, Solid-State Electron. **21**, 43 (1978).